3-D MRI Brain Scan Feature Classification Using an Oct-tree Representation

Akadej Udomchaiporn[1], Frans Coenen[1], Marta García-Fiñana[2], and Vanessa Sluming[3]

[1] Department of Computer Science, University of Liverpool, Liverpool, UK
{akadej,coenen}@liv.ac.uk
[2] Department of Biostatistics, University of Liverpool, Liverpool, UK
m.garciafinana@liv.ac.uk
[3] School of Health Science, University of Liverpool, Liverpool, UK
vanessa.sluming@liv.ac.uk

Abstract. This paper presents a procedure for the classification of specific 3-D features in Magnetic Resonance Imaging (MRI) brain scan volumes. The main contributions of the paper are: (i) a proposed Bounding Box segmentation technique to extract the 3-D features of interest from MRI volumes, (ii) an oct-tree technique to represent the extracted sub-volumes and (iii) a frequent sub-graph mining based feature space mechanism to support classification. The proposed process was evaluated using 210 3-D MRI brain scans of which 105 were from "healthy" people and 105 from epilepsy patients. The features of interest were the left and right ventricles. Both the process and the evaluation are fully described. The results indicate that the proposed process can be effectively used to classify 3-D MRI brain scan features.

Keywords: Image mining, 3-D Magnetic Resonance Imaging (MRI), Image segmentation, Oct-tree representation, Image classification.

1 Introduction

Image mining involves a number of challenges of which the most significant relates to the representation of the image data in a format that allows the effective application of data mining techniques. The nature of the image representation will affect both the efficiency and effectiveness of the data mining. We can divide the domain of image mining into whole image mining and Region Of Interest (ROI) mining where the distinction is that the second is directed as some specific sub-image present across an image collection. In this paper we consider ROI image mining, more specifically we consider 3-D ROI image mining, thus Volume Of Interest (VOI) image mining. We propose a Bounding Box technique to identify specific VOIs within am image collection and an oct-tree formalism with which to represent the identified VOIs. The oct-tree representation in turn can then be processed using a frequent sub-graph mining process which can then be used to generate a feature space that is compatible with the application of data mining (classification) techniques.

To act as a focus for the work we consider 3-D Magnetic Resonance Imaging (MRI) data of the human brain. Note that a 3-D MRI scan comprises a sequence of 2-D "slices". The VOIs in this case are the lateral (left and right) ventricles. The ventricles are fluid-filled open spaces at the centre of the brain; there are four ventricles in a human brain, but in this paper we only consider the lateral ventricles. An example of a 3-D MRI brain scan is shown in Figure 1 where the lateral ventricles are the dark areas at the centre of the brain. The dataset used to evaluate the proposed process was composed of 210 MRI brain scans of which 105 were from "healthy brains" and the remaining 105 were from epilepsy patients. The application goal of the research is to classify MRI brain scans as either epilepsy or non-epilepsy according to the nature of the ventricles (the nature of the lateral ventricles are considered to be indicators of the presence of conditions such as epilepsy). The proposed process is as follow. First we apply our Bounding Box technique to isolate the ventricles. We then represent each ventricle using an oct-tree formalism. A graph mining technique is then used to identify frequently occurring sub-oct-trees. The identified sub-oct-trees are then used to define a feature space from which a feature vector representation can be produced (one vector per image) to which established data mining techniques can be applied.

The rest of the paper is organised as follows. Section 2 introduces some previous work. In Section 3 the classification process is described in detail. The experimental set-up whereby the process was evaluated, and the results obtained, are presented in Sections 4 and 5 respectively. Finally, the paper is concluded in Section 6 with a summary of the main findings.

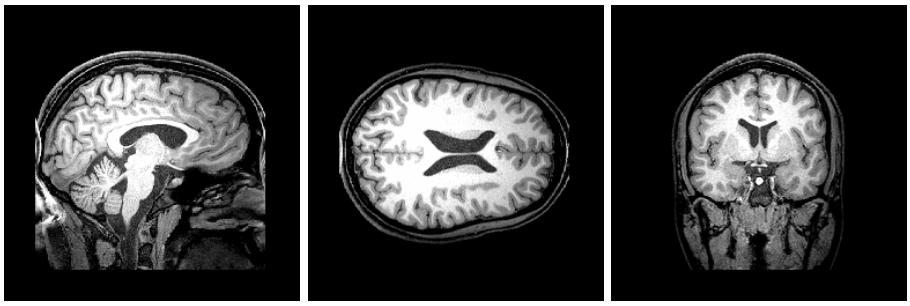

(a) (b) (c)

Fig. 1: Example of a 3-D brain MRI scan: (a) Sagittal (SAG) plane; (b) Transverse (TRA) plane; (c) Coronal (COR) plane

2 Previous Works

Some of the published work on the segmentation of brain images has common aspects with the work described in this paper. For example in [6, 7] a Modified Spectral Segmentation algorithm, founded on a multiscale graph decomposition, was proposed to segment the corpus callosum (another feature present in MRI

brain scans). Experimentation was conducted using 76 MRI data sets; the results indicated that their algorithm could detected the corpus callosum more accurately than when using existing segmentation techniques. However, the work described in [7] was directed at 2-D data (specifically, the *midsagittal* slice of a MRI volume). The work described in [14] is of particular interest with respect to the work described in this paper because they also used an oct-tree conceptualisation from which a feature vector representation was extracted using frequent sib-graph mining. The work described in [14] was also directed at brain ventricles however in the context of Alzheimer's disease. In the context of data capture a technique was presented in [14] to segment both the lateral ventricles and the third ventricles using an oct-tree decomposition, different to that presented in this paper, coupled with a dynamic thresholding technique. This segmentation technique automatically found the most suitable threshold value for each brain image. It was argued that this tended to produce a more accurate result. However, the work described in [14] was focussed on classification accuracy (no evaluation was conducted concerning the segmentation). It is also worth nothing that the process of dynamic thresholding is time consuming. Some other reported work on MRI brain scan segmentation can be found in [17] where a "hand-segmentation" approach was proposed to extract brain ventricles from 3-D MRIs. The approach was implemented using active shape models [3] and level set methods [15]. However, as in the case of [14], no evaluation of the segmentation was included in [15].

Some of the published work on image classification using graph based representations also has common aspects with the work presented in this paper. For instance, in [6] a quad-tree technique was used to represent the corpus callosum. The work also used a frequent sub-graph mining technique to discover frequently occurring sub-graphs in the quad-trees using the well-known Gspan algorithm [18] and the Average Total Weighing (ATW) scheme proposed in [13]. Experiments were conducted to classify MRI brain scans as epilepsy or non-epilepsy (the same application domain as considered in this paper), musicians or non-musicians, and left-handedness or right handedness. With respect to the epilepsy data set a best classification accuracy of 86.32% was obtained; however, as noted above, the technique was only applied in the 2-D context. In the case of [14] (see above) their oct-tree representation technique was used to represent ventricles. The work also used a frequent sub-graph mining algorithm to identify frequently occurring sub-octrees which were then translated into a vector space representation (in a similar manner to that described in this paper). Experiment were conducted to classify individual brain scans with respect to Alzheimer's disease (a dataset of 166 images was used) and with respect to level of education (dataset of 178 images). A best accuracy of 74.2% was obtained for the former and a best accuracy of 77.2% for the latter. To the best knowledge of the authors, there has been a very little work on the application of image mining techniques in the context of ventricles other than that reported in [14] although the latter was directed at the classification of Alzheimer's disease.

3 The Classification Process

Our proposed classification process is illustrated in Figure 2. With reference to the figure a segmentation process is first applied so as to extract the VOI (the lateral ventricles). Secondly an image decomposition process is used to generate oct-trees (one per ventricle). Next frequently occurring sub-graphs are identified and used to define a feature space from which feature vectors are then generated (one per ventricle) using a feature selection mechanism. Any one of a number of classifier generators can then be applied to the feature vector represented data. Each sub-process (indicated by a rectangular box in Figure 2) is described in more detail on the following sub-sections.

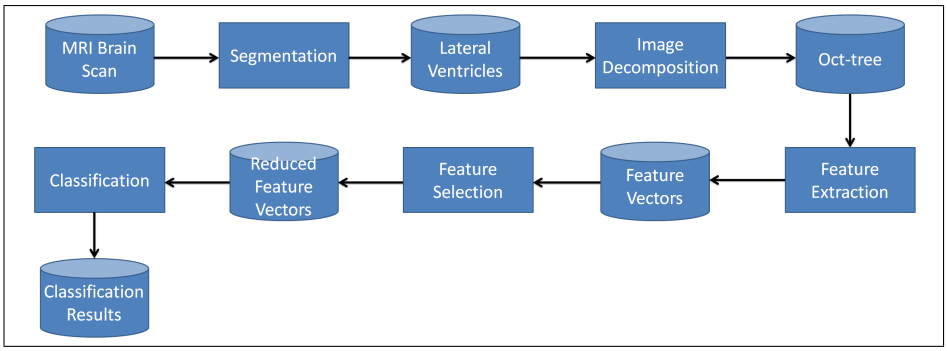

Fig. 2: The Proposed Classification Process

3.1 Segmentation

The identification of VOIs in image data is an important step in image analysis of all kinds. The accuracy with which the nature of a VOI is captured directly affects the effectiveness of any subsequent analysis. The key point of image representation, in the context of data mining, is to remove those elements which will not contribute to the effectiveness of any subsequent analysis, while retaining those that will. In the context of the 3-D MRIs of the human brain used as a focus for the work described in this paper some image preprocessing was first conducted, namely: (i) slice capture and registration, (ii) contrast enhancement.

As indicated in Figure 1, 3-D brain scan MRIs are recorded in three planes: (i) Sagittal (left to right), (ii) Coronal (front to back) and (iii) Transverse (top to bottom). There are a number of software tools which can be used to view and extract slices from 3-D MRI data files. For the work described in this paper the MRICro[1] software system was used. After capturing a collection of image slices, using MRICro, a registration process was applied so that all slices conformed to the same reference framework. Note that the process only requires one set of slices (to evaluate the overall process slices from the Sagittal plane were used).

[1] http://www.mccauslandcenter.sc.edu/mricro/.

For contrast enhancement a thresholding technique [2] was used. This technique is more effective when an object's colours are obviously different to their background colours. However, the technique can still be used in the case where the object and background colours are not noticeably clear. For example, in Figure 3 it can be seen that the ventricles are represented by the dark areas towards the middle of the image, surrounded by brain tissue which appears as grey (or white) matter. Generally, the contrast between the ventricle and other parts of the brain is easily noticeable, but in some slices (such as SAG slice number 160 shown in Figure 3(c)) it is difficult to identify the boundary of the ventricle because there are grey shades within the ventricle area. In this case, the thresholding technique will enhance the contrast so as to aid the identification of the ventricles. During thresholding, each pixel's brightness is compared to a predefined threshold. If the pixel is considered to be part of the VOI the pixel colour is set to some predefined distinguishing colour, otherwise it will be identified as background and set to an alternative predefined colour. The key success of the thresholding process is the selection of the threshold value. In the work described here the image processing suite of functions available in Matlab[2] was used. Using the Matlab suite the threshold value can be automatically assigned by the software or manually set by a human user. With respect to the work described here the selected threshold value was manually set to 0.30. This was selected after the effect of a range of threshold values ($\{0.28, 0.29, 0.31, 0.32, \dots\}$) had been manually observed with respect to a reasonable number of different cases by a domain expert. As a result, if a pixel was darker than 0.30 (of interest) it was set to black, otherwise (not of interest) it was set to white. The brain MRI slices shown in Figure 3 are again shown in Figure 4 after the thresholding technique has been applied.

(a) SAG slice no. 100 (b) SAG slice no. 130 (c) SAG slice no. 160

Fig. 3: Example of brain image slices in the SAG plane

Once the contrast enhancement was complete the VOIs (the verticals) could be segmented. To this end the Bounding Box technique was developed by the authors. This comprised three steps: (i) define a bounding box that is expected to encompass the ventricles of interest with respect to all relevant slices in the given

[2] http://www.mathworks.co.uk/products/matlab/

MRI volume, (ii) for each slice collect the black pixels (voxels) and (iii) apply appropriate noise removal. The required bounding box is rectangular in shape and defined by the coordinates of its corners. To ensure that the bounding box is likely to encompasses all the ventricle voxels of interest it needs to be defined in such a manner that it is considerably larger than the expected ventricle area (so that nothing is missed). All black pixels are collected from each slice that is located within the bounding box. Because the bounding box is defined so that a considerably larger area than the expected ventricle area is covered some black pixels located outside the ventricle area (noise pixels) will also be collected. These are therefore removed in the final step using a simple noise reduction technique whereby the black pixels that are not connected to the largest group of connected pixels are simply removed. In other words the largest group of pixels is assumed to be the ventricles.

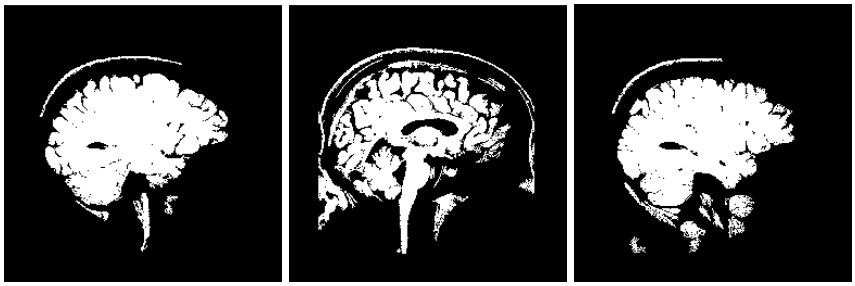

(a) SAG slice no. 100 (b) SAG slice no. 130 (c) SAG slice no. 160

Fig. 4: Example of brain image slices from Figure 3 after applying thresholding (threshold value = 0.30)

To evaluate the proposed Bounding Box segmentation technique experiments were conducted using 85 MRI brain scans. By applying the proposed technique using two sampling directions, two sets of volumes were obtained: (i) in the Sagittal plane and (ii) in the Transverse plane. From the experiments it was found that the volumes obtained were close to those obtained manually. Of course the manually estimated volumes do not provide a "gold standard", and may themselves be flawed due to human error. However they did provide a benchmark. The closest performing technique to the manual technique was found to be when using the Sagittal plane. The results are presented in Figure 5, where the volumes estimated from each technique (mm^3) are plotted according the MRI scan identification numbers sorted according to their associated ventricle size.

The difference in volume (mm^3) between the manual and the proposed techniques against the average is plotted in Figure 6. The mean difference (bias estimate) and the 95% range of agreement (calculated as the mean difference between +2SD and -2SD) is represented by the continuous horizontal lines. From the figure it can be seen that the mean difference between the manually estimated volumes and the volumes collected by the Bounding Box technique when used in the Sagittal plane is the smallest (1.10 mm^3) with a standard devia-

tion of 1.53 mm^3. Note that the difference in volume between the manual and the Bounding Box technique increases as the overall volume of the ventricle increases. Although the proposed techniques produced good results there were some limitations. Firstly, the bounding box had to be initially manually defined thus requiring some resource in order to ensure that the bounding box was not too small. Secondly the technique requires application of a noise removal process which had the effect of increasing the overall runtime of the algorithm. On the positive side the idea behind the technique was simple, easy to implement, and effective. Note that the dataset used in this experiments (comprising 85 MRI brain scans) was a subset of the dataset used in the experiments to evaluate the entire classification process. This was because manual identification of VOIs is a time consuming process hence the authors were only able to manually process 85 MRI brain volumes.

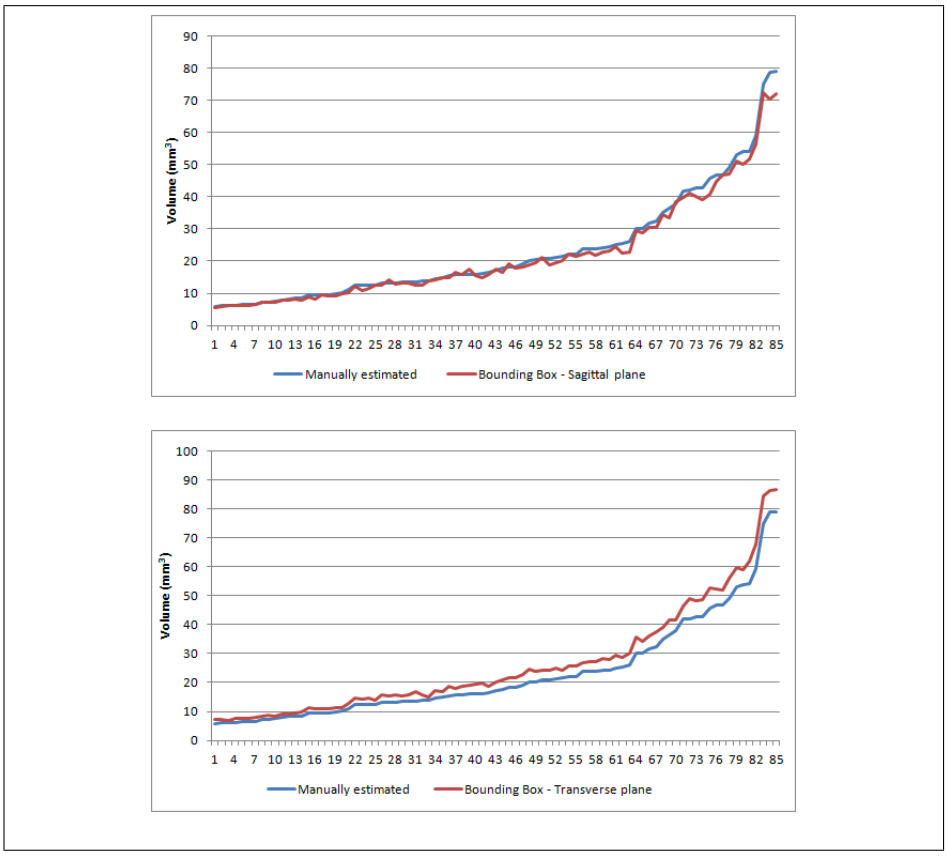

Fig. 5: Comparisons between manually estimated volumes and volumes collected using the proposed automated techniques

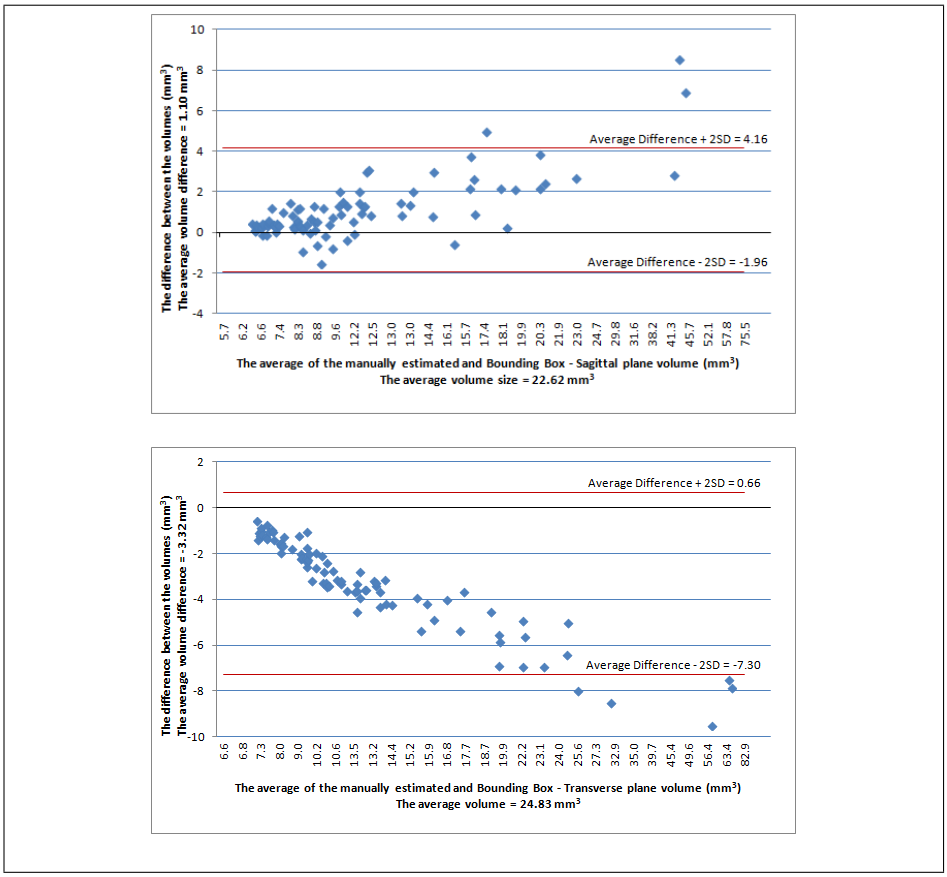

Fig. 6: Levels of agreement in volume estimation between the manual and automated techniques

3.2 Image Decomposition

The objective of image decomposition is to represent an image in some hierarchical format. There are many types of image decomposition, common mechanisms use data structures such as oct-trees, quad-trees and scale space representations [5]. With respect to the work described in this paper, the oct-tree representation was adopted. An oct-tree is a tree data structure which can be used to represent 3-D images that have been recursively subdividing it into eight equal sized octants [12]. Each node in the tree holds image data related to its octant. With respect to the work described in this paper a binary encoding was used. If an octant was part of a ventricle (coloured black) the node was set to 1, otherwise it was set to 0. If an octant did not comprise a homogenous colour it was decomposed further. The process continued until a user defined "maximum depth" was reached. Note that the lateral ventricles consist of two ventricles (left and

right), thus two oct-trees were generated with respect to each image which (for convenience) are joined at the root nodes.

3.3 Feature Extraction, Selection, and Classification

In the final stage of the process the oct-tree represented images are processed further to form a feature vector representation to which standard classification techniques can be applied. This is an idea first proposed in [6, 7] in the context of 2-D MRI brain scans and subsequently used by a number of other researchers such as [9] in the context of 2-D retina images and [14] with respect to 3-D MRI scans. The first element in this part of the process was thus to apply Frequent sub-graph Mining (FSM) to the oct-tree data. A number of FSM algorithms have been proposed, such as: (i) Gspan [18], (ii) AGM [11], and (iii) FFSM [10]. The Gspan algorithm was used with respect to the work described here. The output of FSM is a set frequently occurring sub-graphs together with their occurrence counts. Typically a large number of sub-graphs are generated many of which are redundant (do not serve to discriminate between classes). Feature selection techniques are typically used to reduce the overall number of identified frequent sub-graphs. With respect to the work presented in this paper the feature selection mechanisms available within the Waikato Environment Knowledge Analysis (WEKA) data mining workbench [8] were used.

4 Experimentation

This section described the experimental set up used to evaluate the proposed process described above (the results obtained are presented in Section 5 below). The experimentation was conducted using three classification methods: (i) Naive Bayes [1], (ii) Support Vector Machine (SVM) [4], and (iii) Decision Trees (C4.5) [16]. All of them are provided within WEKA [8]. With respect to the Gspan algorithm four different minimum support thresholds were used to define frequent sub-graphs ($\{20\%, 30\%, 40\%, 50\%\}$). As a result, four sets of feature vectors were generated and used as inputs for each classifier. Results were produced using Ten-fold Cross Validation (TCV). Recall from the introduction to this paper that the image set used for evaluation purposes comprised 210 MRIs obtained from the Magnetic Resonance and Image Analysis Research Centre at the University of Liverpool. Each scan consisted of 256 two dimensional (2-D) parallel image slices in each plane. The "resolution" of each image slice was 256 x 256 pixels with colour defined using an 8-bit gray scale (thus 256 colours). This was the same data set as used by El Sayed et al. as reported in [7], however El Sayed et al. investigated the potential of the corpus callosum as an indicator of epilepsy (as opposed of the ventricles) and only considered 2-D representations.

5 The Classification Results

The classification results obtained are shown in Table 1. The metrics used to evaluate performance of the classification methods are accuracy (Accu.), sensi-

tivity (Sens.) and Specificity (Spec.). The T values in the first column are the Gspan minimum support thresholds. From Table 1 it can be seen that the best classification accuracy was from the SVM classifier coupled with $T = 30\%$, while the worst was obtained using Naive Bayes coupled with $T = 50\%$. The relation between classification accuracy and support threshold for each classifier is shown in the graph presented in Figure 7. From the graph it is obvious that the best classifier for this dataset is SVM, and the best support threshold is $T = 30\%$. The classification accuracy with respect to all the classifiers considered tended to decrease as the support threshold increased. It was conjectured that this was because significant sub-graphs were not discovered using Gspan when high support thresholds were adopted.

Table 1: Classification results obtained using Naive Bayes, Support Vector Machine (SVM), and Decision Trees

	Naive Bayes			SVM			Decision Trees		
T(%)	Accu.	Sens.	Spec.	Accu.	Sens.	Spec.	Accu.	Sens.	Spec.
20	64.34	67.25	66.80	68.53	70.40	68.23	67.83	70.58	68.67
30	68.53	70.40	69.23	72.34	75.67	70.45	70.45	74.28	73.20
40	65.13	68.57	70.34	70.45	72.34	69.23	65.87	70.47	65.40
50	61.56	65.40	64.15	62.28	66.96	60.67	62.80	67.05	64.15

6 Conclusions

In this paper an approach to 3-D MRI brain scan feature classification has been proposed. The main contributions were the Bounding Box segmentation technique, the oct-tree representation technique and the use of FSM to identify features. In the reported experimental study the Bounding Box technique when applied in the Sagittal plane produced the best segmentation outcomes. In the context of the overall proposed classification process (using the oct-tree representation and FSM) promising outcomes were produced. The results reported in [7] were better than those reported here, however the work in [7] was directed at a 2-D representation of the corpus callosum which may be a better indicator of epilepsy. Likewise, despite using a similar technique, the results reported in [14] were slightly better than those reported in this paper. However, the work in [14] considered not only the lateral but also the "third" ventricle. Moreover, the datasets in [14] (Alzheimer's disease and level of education) were different to those used in this paper. The lateral and third ventricles may be better indicators of Alzheimer's disease and level of education than epilepsy.

The next stage of our research will focus on alternative methods of representing 3-D MRI brain scan features so that machine learning techniques can be applied. The intention is also to consider the use of dynamic thresholding techniques, as used in [14], to determine whether this helps improve the effectiveness of the segmentation process. Regarding the classification process some weighting technique (such as that proposed in [13]) could be applied to the FSM process in order to improve its operation.

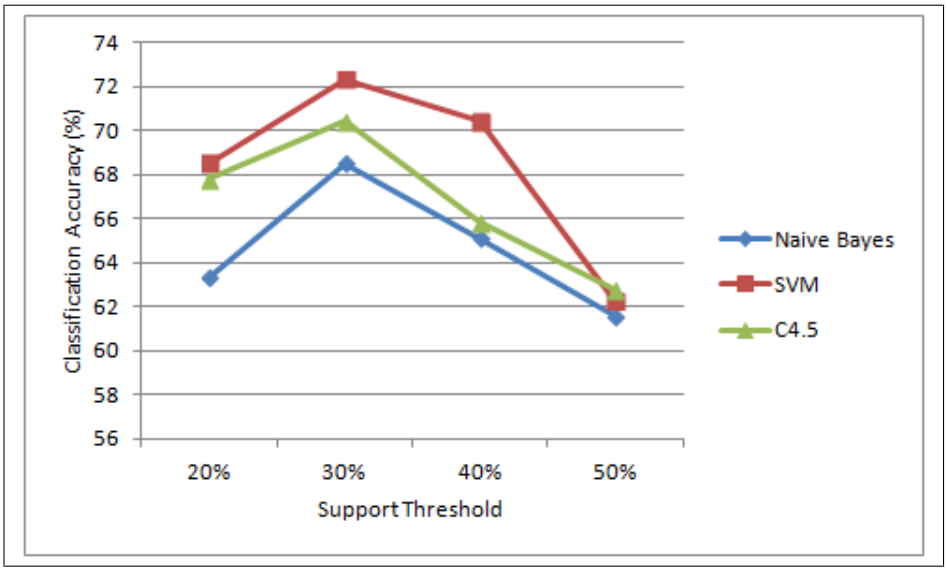

Fig. 7: Relation between classification accuracy and support threshold for each classifier

References

1. M. Bramer. *Principles of Data Mining*. Springer, 2007.
2. W. Burger and M. J. Burge. *Digital Image Processing: An algorithmic Introduction Using Java*. Springer, 2008.
3. T. Cootes, C. Taylor, D. Cooper, and J. Graham. Active shape models-their training and application. *Computer Vision and Image Understanding*, 61(1):38 – 59, 1995.
4. C. Cortes and V. Vapnik. Support-vector Networks. *Machine Learning*, 20(3):273–297, 1995.
5. L. D. F. Costa and R. M. C. Jr. *Shape Analysis and Classification: Theory and Practice*. CRC Press, 2001.
6. A. Elsayed, F. Coenen, C. Jiang, M. García-Fiñana, and V. Sluming. Corpus Callosum MR Image Classification. In *Proceedings AI'09*, pages 333–348. Springer, 2009.
7. A. Elsayed, F. Coenen, C. Jiang, M. García-Fiñana, and V. Sluming. Corpus Callosum MR Image Classification. *Knowledge-Based Systems*, 23(4):330–336, May 2010.
8. M. Hall, E. Frank, and G. Holmes. The WEKA Data Mining Software: An Update. *ACM SIGKDD Explorations Newsletter*, 11(1):10–18, 2009.
9. M. Hijazi, F. Coenen, and Y. Zheng. Image Classification for Age-related Macular Degeneration Screening using Hierarchical Image Decompositions and Graph Mining. In *ECML PKDD 2011*, pages 65–80. Springer LNAI6912, 2011.
10. J. Huan, W. Wang, and J. Prins. Efficient Mining of Frequent Subgraphs in the Presence of Isomorphism. In *Proceedings of The Third IEEE International Conference on Data Mining*, pages 549–552. IEEE Comput. Soc, 2003.

11. A. Inokushi, T. Washio, and H. Motoda. An Apriori-based Algorithm for Mining Frequent Substructure from Graph Data. In *Proceedings of the Forth European Conference on Principles and Practice of Knowledge Discovery in Database*, pages 13–23, 2000.
12. C. L. Jackins and S. L. Tanimoto. Oct-trees and Their Use in Representing Three-dimensional Objects. *Computer Graphics and Image Processing*, 14(3):249–270, Nov. 1980.
13. C. Jiang and F. Coenen. Graph-based Image Classification by Weighting Scheme. In *Applications and Innovations in Intelligent System XVI*, pages 63–76. 2009.
14. S. Long and H. L. B. Graph-based Shape Shape Analysis for MRI Classification. *International Journal of Knowledge Discovery in Bioinformatics*, 2(2):19–33, 2011.
15. S. Osher and J. A. Sethian. Fronts Propagating with Curvature-Dependent Speed: Algorithms Based on Hamilton-Jacobi Formulations. *Journal of Computational Physics*, 79(1):12–49, Nov. 1988.
16. J. R. Quinlan. *C4.5: Programs for Machine Learning*. Morgan Kaufmann Publishers, 1993.
17. M. Rousson, N. Paragios, and D. Rachid. Implicit Active Shape Models for 3-D Segmentation for MR Imaging. In *Medical Image Computing and Computer-Assisted Intervention*, pages 209–216, 2004.
18. X. Yan. gSpan: Graph-based Substructure Pattern Mining. In *Proceeding of The IEEE International Conference on Data Mining*, pages 721–724. IEEE Comput. Soc, 2002.